Journal of Physics: Condensed
Matter

PAPER • OPEN ACCESS

Chemo-elasto-electro free energy of non-uniform system in the diffuse interface context

To cite this article: Yuhan Cai *et al* 2024 *J. Phys.: Condens. Matter* **36** 495702

OPEN ACCESS
IOP Publishing
Journal of Physics: Condensed Matter
J. Phys.: Condens. Matter **36** (2024) 495702 (12pp)
https://doi.org/10.1088/1361-648X/ad7660

Chemo-elasto-electro free energy of non-uniform system in the diffuse interface context

Yuhan Cai[1], **Fei Wang**[1,2,*], **Haodong Zhang**[2] **and Britta Nestler**[1,2,3]

[1] Institute of Applied Materials-Microstructure Modelling and Simulation, Karlsruhe Institute of Technology (KIT), Straße am Forum 7, 76131 Karlsruhe, Germany
[2] Institute of Nanotechnology, Karlsruhe Institute of Technology (KIT), Hermann-von-Helmholtz-Platz 1, 76344 Eggenstein-Leopoldshafen, Germany
[3] Institute of Digital Materials Science, Karlsruhe University of Applied Sciences, Moltkestraße 30, 76133 Karlsruhe, Germany

E-mail: fei.wang@kit.edu

Received 9 July 2024, revised 23 August 2024
Accepted for publication 2 September 2024
Published 12 September 2024

Abstract

In the present work, we propose an alternative approach for deriving the free energy formulation of a non-uniform system. Compared with the work of Cahn and Hilliard (1958 J. *Chem. Phys.* **28** 258–67), our approach provides a more comprehensive explanation for the individual energy contribution in a non-uniform system, including entropy, interaction energy, and internal energy. By employing a fundamental mathematical calculus, we reformulate the local composition within the interface region. Utilizing the reformulated local composition as well as classic thermodynamic principles, we establish formal expressions for entropy, interaction energy, and the internal energy, which are functions of both composition and composition gradients. We obtain a comprehensive free energy expression for a non-uniform system by integrating these energy density formulations. The obtained free energy expression is consistent with the formula type of Cahn and Hilliard and prodives more deeper physical interpretation. Moreover, using the same approach, we derive formulations for elastic energy and electric potential energy in a non-uniform system. However, the proposed approach encounters a limitation in the special case of a non-uniform fluid contacting a solid substrate. Due to the significant difference in the length scales between the solid–fluid and fluid–fluid interfaces, the wall free energy formulation based on the aforementioned concept is unsuitable for this multi-scale system. To address this limitation, we reformulate the wall free energy as a function of the average composition over the solid–fluid interface. Additionally, the previous derivation relies on an artificial treatment of describing the composition variation across the interface by a smooth monotone function, while the true nature of this variation remains unclear. By utilizing the concept of average composition, we circumvent the open question of how the composition varies across the interface region. Our work provides a thorough understanding for the construction of free energy formulations for a non-uniform system in condensed matter physics.

---

[*] Author to whom any correspondence should be addressed.

Keywords: free energy formulation, non-uniform system, diffuse interface model, thermodynamics

List of symbols

Notation	**Description**
Ω	Domain investigated
S	Domain boundary
$\mathcal{F}$	Chemical free energy functional
ρ	Density
h	Distance between the separation layer and the middle of the liquid
ω	Successive factor
θ	Orientation angle
R	Anisotropic interfacial energy
ψ	Inclination of the normal to the liquid–solid interface with respect to the growth direction
α	Gradient energy coefficient
φ	Phase parameter
z	Coefficient controlling the coupling strength between φ and $\nabla\theta$
e	Coefficient controlling the coupling strength between φ and $\nabla\theta$
m	Local magnetization variable
$\tilde{K}$	Coefficient proportional to the interaction energy and to the number of lattice bonds
f_0	Free energy density of uniform system
κ	Coefficient of the gradient term in free energy formulation
f	Chemical free energy density
c_i	Volume fraction of the ith component
K	Number of the components
N_A	Avogadro constant
R_g	Gas constant
n_i	Mole numbers of the ith component
v_i	Molar volume of the ith component
$\bar{v}$	Average molar volume of system
T	Temperature
P	Pressure
$\mathcal{S}_B$	Configurational entropy functional
s_B	Configurational entropy density
k_b	Boltzmann constant
W	Number of the configurations
λ	Interfacial length
$\boldsymbol{\ell}_i$	Characteristic length vector of ith component of liquid
$\mathbf{m}$	Outer normal vector of the domain boundary
h_B	Interaction energy density
$\mathcal{H}$	Interaction energy functional
χ_{ij}	Interaction coefficients between ith and jth components
u	Internal energy density
C_v	Heat capacity
$\mathcal{U}$	Internal energy
$\mathcal{S}$	Entropy functional
s	Entropy density
Γ	Diffuse-interface region that liquid interacts with the solid substrate
Γ'	Sharp-interface boundary that liquid interacts with the solid substrate
$\mathcal{F}_\mathrm{W}$	Wall energy functional
c_s	Solid substrate composition
$\boldsymbol{\ell}_s$	Characteristic length vector of solid substrate
$\bar{c}_i$	average composition of ith component in substrate–fluid interface
f_E	Elastic energy density
$\mathcal{F}_\mathrm{E}$	Elastic energy functional
$\boldsymbol{\epsilon}$	Strain tensor
$\boldsymbol{C}$	Elasticity tensor
$\mathcal{U}_\mathrm{E}$	Electric potential energy
ε	Permittivity
$\boldsymbol{E}$	Electric field strength

1. Introduction

Classical Newton's laws of motion describe the relationship between the motion of a mass object and the forces acting on it. Newton applied these laws to investigate and to explain the motion of many physical objects and systems. During this period, the concept of energy emerged in the minds of researchers, such as Leibniz, Bacon, and Newton, leading to new insights that laid the foundation for classical mechanics. However, Newton's laws have limitations when applied to very large systems consisting of many particles, such as one mole of water, which is composed of approximately 6×10^{23} water molecules. With the development of thermodynamics, particularly statistical thermodynamics, researchers surpassed these limitations. Statistical thermodynamics, based on atomic and molecular theories, relates the microscopic properties of individual atoms and molecules to the macroscopic properties of materials. For instance, Gibbs described the energy of systems with a uniform composition (see figures 1(a) and (b)) by integrating the energy density over the whole domain Ω as

$$\mathcal{F} = \int_\Omega f(c)\,\mathrm{d}\Omega, \tag{1}$$

where $f(c)$ is the free energy density related to the composition c. However, non-uniform systems, such as multicomponent alloys or water-oil mixtures, are more common in the real world. In these non-uniform systems, physical quantities vary across separation layers, known as interfaces. The study of interfacial phenomena in materials science has attracted great attention of researchers over the past two centuries. Understanding and controlling interfacial phenomena is essential for optimizing material properties, designing advanced materials, and developing innovative technologies across various fields. Over time, the understanding of physical interfaces has become deeper and clearer. In the early 19th century, some researchers, such as Young and Laplace, conceptualized fluid interfaces as surfaces of zero thickness. These foundational studies, primarily rooted in static or mechanical equilibrium considerations, posited that key physical quantities like density could exhibit discontinuities across the interface. Processes like capillarity at fluid interfaces are characterized by specific boundary conditions, notably encapsulated in Young's equation [1] for the equilibrium contact angle or the Young–Laplace equation linking pressure differences across an interface to surface tension and curvature. Several decades later, researchers such as Poisson, Maxwell, and Gibbs recognized that physical quantities change rapidly but smoothly across the interface between two bulk phases. Among them, Gibbs [2] introduced the concept of dividing surface and surface excess quantities, which facilitate in the development of equilibrium thermodynamics principles for interfaces. Although Gibbs recognized the existence of a dividing surface between different phases, the description of the energy within this dividing surface still has a gap. Motivated by these previous investigations, Rayleigh and van der Waals further developed the idea of interface with non-zero thickness in detail, proposing gradient theories for the interface science based on thermodynamic principles. In particular, van der Waals [3] proposed the concept of 'diffuse interface' and gave a theory to predict its thickness. In van der Waals's theory, the thickness of this layer increases with rising temperature and becomes infinite as the critical temperature is approached.

In inhomogeneous systems, well-defined phases are separated by thin interfaces. The formation and movement of the interface are often observed in physical processes, for example, phase separation and solidification. Phase separation and solidification are fundamental processes in materials science and engineering, influencing the formation of microstructures and properties of materials. Understanding these phenomena requires accurate modeling approaches that capture the evolution of interfaces between different phases. Advanced analytical techniques enable detailed investigations of interfacial behavior, leading to insights that drive material innovation and technological progress. With the development of the modern computer, computational modeling becomes an outstanding research method in these investigations.

Today, the diffuse interface model serves as a powerful computational tool for simulating interfacial phenomena at the mesoscale, including phase separation [4–7], solidification [8–10], grain boundary grooving [11], wetting behavior [12], to name a few. Unlike the sharp-interface model, the diffuse interface model represents phase boundaries as gradual transitions over a finite region, eliminating the need to explicitly track the interface position. In cases where phases deviate from equilibrium, one phase grows at the expense of others. Specifically, the interface undergoes movement until the non-equilibrium system reaches a state of thermodynamic equilibrium. In this model, variable order parameters vary smoothly across the interface between two distinct phases, reflecting changes in physical properties. For example, van der Waals considered the liquid–vapor interface and assumed that the separation surface is horizontal. In this case, the total energy of the system is formulated as a function of the density [3]:

$$\mathcal{F} = \int \rho \left[f(\rho) - \frac{\omega}{2} \frac{\mathrm{d}^2 \rho}{\mathrm{d}h^2} \right] \mathrm{d}h, \tag{2}$$

where ρ indicates the density and exhibits a continuous variation through the boundary layer, h is the distance between the separation layer and the middle of the liquid, ω represents a successive factor, and $f(\rho)$ depicts the free energy in surroundings of homogeneous density. In the studies of the crystal growth, Warren *et al* [13, 14] introduced the orientation angle of the crystalline grain θ as a new order parameter to reflect the degree of orientational order as well as the predominant local orientation of the crystal. They described the free energy that includes crystallographic orientation fields as:

$$\mathcal{F} = \int_\Omega \left[f(\varphi, T) + \frac{\alpha^2}{2} R^2 \left(|\nabla\varphi|, \theta - \psi \right) + z g(\varphi) |\nabla\theta| + \frac{e^2}{2} h(\varphi) |\nabla\theta|^2 \right] \mathrm{d}\Omega, \tag{3}$$

where z and e control the strength of the coupling between φ and $\nabla\theta$, R depicts the anisotropic interfacial energy, and ψ is the inclination of the normal to the liquid–solid interface with respect to the growth direction. α is the gradient energy coefficient determining the magnitude of the penalty induced by the presence of interfaces. The two functions, $g(\varphi)$ and $h(\varphi)$, both are monotonic with respect to the phase parameter φ. Obeying the basic law of thermodynamics, the minimization of the total energy in the system yields the dynamic equations governing the temporal and spatial evolution of the order parameters. The Ginzburg–Landau equation [15] and the Cahn–Hilliard equation [16] are the two most familiar examples, which are widely applied in the studies of the interfacial phenomenon with phase-field method. The standard derivation of these two equations is based on the total energy formulation of a non-uniform system proposed by Cahn and Hilliard [16]. Based on the understanding of the diffuse interface, they derived a general equation for the energy of a non-uniform system, which has a spatial variation in composition. The chemical free energy functional of the system over the domain Ω occupied by the material is expressed as:

$$\mathcal{F} = \int_\Omega f(c, \nabla c, \cdots) \, \mathrm{d}\Omega. \tag{4}$$

In this formulation, the chemical free energy density is a continuous function of composition and its gradient. It can be expanded in a Taylor series referring to f_0, which represents the free energy of a solution with a uniform composition c. A general expression for a non-uniform system is obtained without the terms in derivatives higher than the second:

$$\mathcal{F} = \int_\Omega \left[f_0 + \kappa (\nabla c)^2 \right] \mathrm{d}\Omega, \tag{5}$$

where

$$\kappa = -\left[\partial^2 f / \left(\partial c \, \partial \nabla^2 c \right) \right]_0 + \left[\partial^2 f / \left(\partial |\nabla c| \right)^2 \right]_0 .$$

Here, the subscript zero indicates the value of the parameter in a solution of uniform composition. This expression consists of an integral comprising two components: the bulk energy term, which describes the energy contribution from the homogeneous part of the system and depends solely on the local composition; and the gradient energy term, which accounts for the energy contribution from the interface and depends on the local composition gradient. This diffuse interface model has been widely applied in researches over several decades. Plapp [17] derived diffuse-interface equations for two simple lattice models: the Ising model, which describes the ferromagnetic to paramagnetic transition, and a binary lattice alloy model. By using mean-field approximations in further derivation, Plapp obtained the coarse-grained free energy in Ginzburg–Landau form:

$$\mathcal{F} = \int_{\Omega} \left[f(m) + \frac{\tilde{K}}{2} (\nabla m)^2 \right] \mathrm{d}\Omega, \tag{6}$$

where the constant $\tilde{K}$ is proportional to the interaction energy and to the number of lattice bonds between neighboring cells, and $f(m)$ represents the local free energy density for a single coarse-grain cell related to the local magnetization variable m. In this work, Plapp indicated that the origin of the gradient term is due to the interactions between neighboring coarse-grain cells in this context. The mathematical validity of this derivation is well-established. However, the standard energy formulation proposed by Cahn and Hilliard still has several limitations:

- The Cahn–Hilliard model is primarily tailored for binary systems, assuming a simplified form of the free energy. This simplification may not adequately capture the complex interactions in multi-component systems, thereby limiting its predictive accuracy in a more general scenario.
- The derivation of the Cahn–Hilliard formulation relies on a Taylor expansion of the total free energy around a specific composition. However, this approach does not explicitly account for the individual contributions of entropy, interaction energy, and internal energy.
- The standard formulation predominantly considers the chemical free energy contribution, neglecting other potential energy components, such as elastic energy or electrostatic potential energy. This omission constrains the model's applicability to systems, where these additional energy terms play a significant role.
- The Cahn–Hilliard framework is inherently limited in addressing multi-scale problems, particularly those that require coupling between different physical phenomena across varying length scales.

To better understand the diffuse interface model and address the aforementioned limitations, a more comprehensive exploration of the gradient term in the free energy formulation for non-uniform systems is essential. In the present study, we begin with the mixing entropy formulation of the system and subsequently consider the interaction energy for the system with immiscible phases. Through straightforward mathematical derivation, we obtain an energy formulation for a 'non-uniform' system that aligns with the expression of Cahn and Hilliard [16] and explain the physical significance of the interfacial energy term in this formulation. Furthermore, we derive formulations for other possible energy contributions in a non-uniform system, such as elastic potential energy and electric potential energy. In the special case of a non-uniform fluid contacting a solid substrate, such as in wetting phenomena, we reformulate the wall free energy as a function of the average composition within the substrate–fluid interface, rather than relying on the local composition and composition gradient. This reformulated wall free energy can be applied to study the multiscale system, which arises due to the different length scales of the substrate–fluid interface and the fluid–fluid interfaces. This approach also avoids an open question of describing the composition variation of one component across the interface region.

2. An alternative concept

In the following discussion, our derivation is based on the lattice model for a system consisting of K components. We define the volume fraction of the ith component as

$$c_i = \frac{n_i v_i}{\sum_{i=1}^{K} n_i v_i}, \tag{7}$$

where n_i and v_i are the moles and molar volume of the ith component, respectively. According to definition, the constraint: $\sum_{i=1}^{K} c_i = 1$ must be satisfied.

As schematically illustrated in figures 1(a) and (b), a uniform system has a homogeneous composition and its free energy density depends solely on compositions, namely $f(c_i)$. In the non-uniform system, the composition changes from one bulk value to another, as shown in figures 1(c) and (d). Therefore, the formulation of its free energy should differ from that of a uniform system. According to the work of Cahn and Hilliard, as mentioned in introduction, the free energy density of a non-uniform system is directly expressed as the function of composition as well as its derivative $f(c_i, \nabla c_i)$. The final expression of the free energy is obtained by expanding the free energy density in a Taylor series without the terms in derivatives higher than the second.

In the present work, we propose an alternative concept for deriving the free energy formulation of non-uniform systems. Our derivation begins with the reformulation of the local composition in the interface region. As illustrated by the dashed rectangle in figure 1(d), the unit domain characterized by composition c_i includes not only the bulk contribution but also contributions from boundary layers. At the left and right boundary layers, the compositions are denoted as c_i^+ and c_i^-, respectively. The composition at two boundary layers are formulated as:

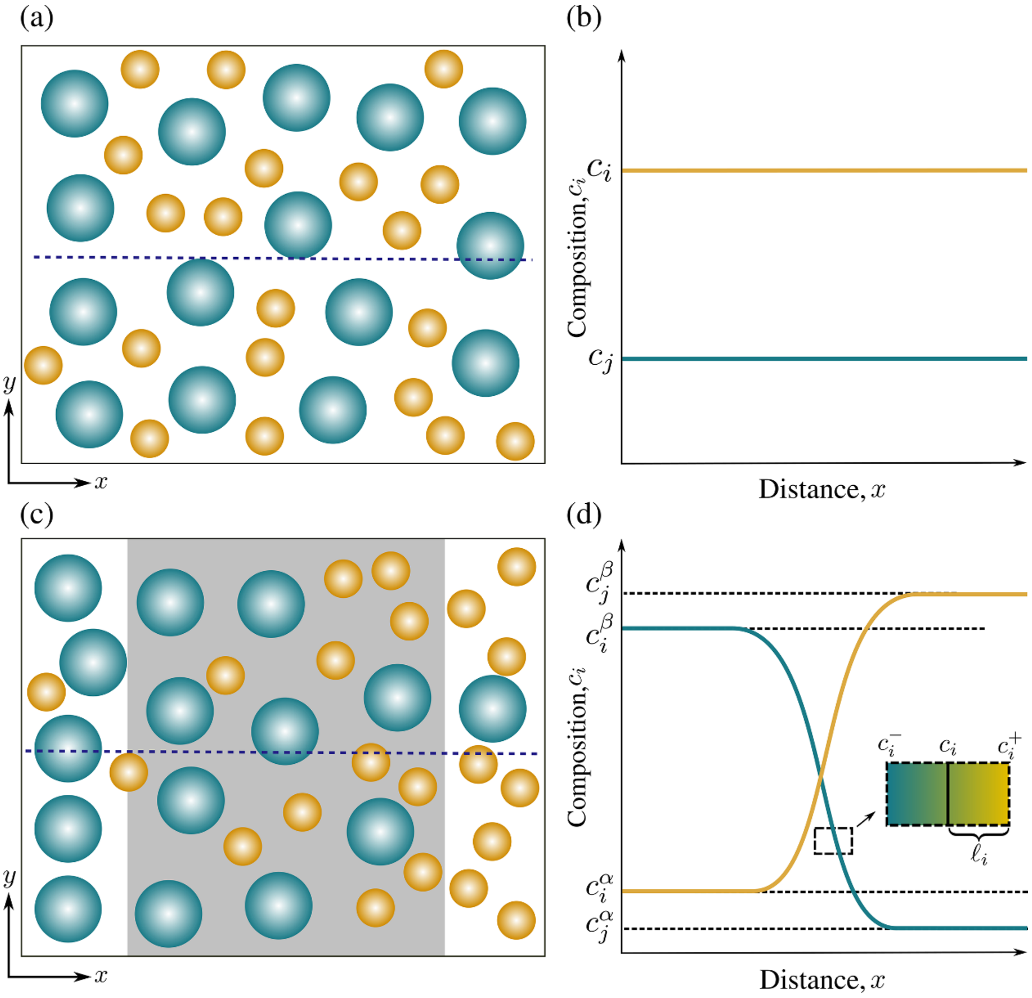

Figure 1. (a) and (c) Schematic illustrations of random mixing of elements, marked by dark green and yellow circles, in a uniform and non-uniform binary system, respectively. (b) and (d) The corresponding concentration profiles of uniform and non-uniform system along the black dashed lines in (a) and (c). The gray region in (c) represents the interface region. The dashed rectangle in (d) indicates the unit domain characterized by composition c_i in the interface region. The compositions at two boundaries of this domain are denoted as c_i^+ and c_i^- and ℓ_i is the characteristic length.

$$c_i^\pm \approx c_i \pm \nabla c_i \cdot (\boldsymbol{\ell}_i)^\mathrm{T} + (\boldsymbol{\ell}_i) \cdot \begin{bmatrix} \frac{\partial^2 c_i}{\partial x^2} & \frac{\partial^2 c_i}{\partial x \partial y} & \frac{\partial^2 c_i}{\partial x \partial z} \\ \frac{\partial^2 c_i}{\partial y \partial x} & \frac{\partial^2 c_i}{\partial y^2} & \frac{\partial^2 c_i}{\partial y \partial z} \\ \frac{\partial^2 c_i}{\partial z \partial x} & \frac{\partial^2 c_i}{\partial z \partial y} & \frac{\partial^2 c_i}{\partial z^2} \end{bmatrix} \cdot (\boldsymbol{\ell}_i)^\mathrm{T}, \tag{8}$$

considering the first- and second-order infinitesimal increments in composition. This expression is derived from a second-order Taylor series expansion of the concentration profile around a point within the interface. The first term indicates the concentration at the reference point within the interface. The second term describes the linear variation in concentration in the direction of $\boldsymbol{\ell}_i$, reflecting how concentration changes along that vector. The third term accounts for the second-order effects, capturing the curvature in the concentration profile within the interface. Here, x, y, z represent the space coordinate and $\boldsymbol{\ell}_i$ indicates a characteristic length vector of ith component describing the length and direction of its variation within the interface region. Due to varying intermolecular interactions, such as attraction and repulsion, the characteristic length scale $\boldsymbol{\ell}_i$ is different for distinct species. Since $\boldsymbol{\ell}_i$ should be isotropic for liquids,

$$\begin{bmatrix} \frac{\partial^2 c_i}{\partial x^2} & \frac{\partial^2 c_i}{\partial x \partial y} & \frac{\partial^2 c_i}{\partial x \partial z} \\ \frac{\partial^2 c_i}{\partial y \partial x} & \frac{\partial^2 c_i}{\partial y^2} & \frac{\partial^2 c_i}{\partial y \partial z} \\ \frac{\partial^2 c_i}{\partial z \partial x} & \frac{\partial^2 c_i}{\partial z \partial y} & \frac{\partial^2 c_i}{\partial z^2} \end{bmatrix} = \begin{bmatrix} \frac{\partial^2 c_i}{\partial x^2} & 0 & 0 \\ 0 & \frac{\partial^2 c_i}{\partial y^2} & 0 \\ 0 & 0 & \frac{\partial^2 c_i}{\partial z^2} \end{bmatrix} \tag{9}$$

is a diagonal matrix and equation (8) can be simplified as

$$c_i^\pm \approx c_i \pm \nabla c_i \cdot \boldsymbol{\ell}_i + \nabla^2 c_i \left(\boldsymbol{\ell}_i\right)^2. \tag{10}$$

3. Entropy formulation of non-uniform system

For pure substance systems, the entropy density is a function of the internal energy density, which depends solely on temperature. When a system consists of more than one component, the entropy density s has an additional dependence on the composition $\boldsymbol{c} = (c_1, c_2, \ldots, c_K)$. For a homogeneous system, the components are fully miscible with each other, the configuration entropy functional $\mathcal{S}_B$ of the system is obtained by integrating the entropy density s_B over the domain Ω as

$$\mathcal{S}_B = \int_\Omega s_B(\boldsymbol{c})\,\mathrm{d}\Omega. \tag{11}$$

The configuration entropy density at a constant temperature T can be calculated by using the Boltzmann equation as

$$s_B = -\frac{k_\mathrm{b} N_\mathrm{A}}{\bar{v}} \ln W, \tag{12}$$

where k_b represents the Boltzmann constant, N_A is the Avogadro constant, and $\bar{v}$ indicates the average molar volume of the system. The number of configurations W for a mixture is counted by using the formula for permutations:

$$W = \frac{N!}{\prod_{i=1}^{K} n_i!}, \tag{13}$$

where $N = \sum_{i=1}^{K} n_i$ (n_i is the moles of component i) and $N!$ denotes factorial of N. In this case, the entropy density s_B is uniform across the domain Ω, when the temperature T and pressure P exhibit uniformity. By considering a lattice model and applying the Stirling's formula, we have

$$s_B(\boldsymbol{c}) = -\frac{k_\mathrm{b} N_\mathrm{A}}{\bar{v}} \sum_{i=1}^{K} c_i \ln c_i. \tag{14}$$

However, for a system consisting of immiscible phases, there exists a *physical* diffuse-interface characterized by an interfacial length denoted as λ, typically on the nanometer scale [18, 19]. Across this interface, the composition c_i is assumed to change smoothly from one bulk equilibrium value to the other. Typical examples include systems such as water-oil [20], water-air [21], and immiscible alloy [22]. In this case, the entropy formulation needs to be amended compared to the bulk formulation given by equation (14). Substituting equation (10) into the Boltzmann equation, the entropy density is expressed as

$$s_B = -\frac{1}{2}\frac{k_\mathrm{b} N_\mathrm{A}}{\bar{v}} \sum_{i=1}^{K} \left(c_i^- \ln c_i^- + c_i^+ \ln c_i^+\right). \tag{15}$$

The factor $1/2$ accounts for the fact that the boundary is also shared with a neighboring cell. By employing the Taylor expansion for the infinitesimal increment of composition, we obtain the following expression for the entropy density

$$s_B(\boldsymbol{c}) = -\frac{k_\mathrm{b} N_\mathrm{A}}{\bar{v}} \sum_{i=1}^{K} \Big[c_i \ln c_i + \frac{1}{2c_i} (\boldsymbol{\ell}_i)^2 (\nabla c_i)^2 + (1+\ln c_i)\nabla^2 c_i\, (\boldsymbol{\ell}_i)^2 + \mathcal{O}\left(\Delta c_i^4\right) \Big]. \tag{16}$$

Substituting equation (16) into equation (11) and applying the divergence theorem

$$\int_\Omega (1+\ln c_i)\nabla^2 c_i\,\mathrm{d}\Omega = -\int_\Omega \nabla(1+\ln c_i)\cdot\nabla c_i\,\mathrm{d}\Omega + \int_S (1+\ln c_i)\nabla c_i\cdot\mathbf{m}\,\mathrm{d}S \tag{17}$$

and no-flux boundary condition $\nabla c_i \cdot \mathbf{m} = 0$ ($\mathbf{m}$ indicates the outer normal vector of the domain boundary S), $\mathcal{S}_B$ is reformulated as:

$$\begin{aligned}\mathcal{S}_B &= \int_\Omega -\frac{k_\mathrm{b} N_\mathrm{A}}{\bar{v}} \sum_{i=1}^{K} \Bigg[c_i \ln c_i + \underbrace{\frac{1}{2c_i}}_{=:\kappa_1^s} (\boldsymbol{\ell}_i)^2 (\nabla c_i)^2 - \underbrace{\frac{\mathrm{d}(1+\ln c_i)}{\mathrm{d}c_i}}_{=:\kappa_2^s} (\boldsymbol{\ell}_i)^2 (\nabla c_i)^2 \Bigg] \mathrm{d}\Omega \\ &= \int_\Omega -\frac{k_\mathrm{b} N_\mathrm{A}}{\bar{v}} \sum_{i=1}^{K} \left[c_i \ln c_i - \frac{1}{2c_i} (\boldsymbol{\ell}_i)^2 (\nabla c_i)^2 \right] \mathrm{d}\Omega, \end{aligned} \tag{18}$$

where the cut-off terms are ignored. By using the definition of the gas constant $R_\mathrm{g} = N_\mathrm{A} k_\mathrm{b}$, the equation (18) can be expressed as

$$\mathcal{S}_B = \int_\Omega -\frac{R_\mathrm{g}}{\bar{v}} \sum_{i=1}^{K} \left[c_i \ln c_i - \frac{1}{2c_i} (\boldsymbol{\ell}_i)^2 (\nabla c_i)^2 \right] \mathrm{d}\Omega. \tag{19}$$

It is evident that the entropy for the immiscible phases (equation (19)) is consistent with the entropy for the fully miscible case, when there is no composition gradient, i.e. $\nabla c_i = 0$, $\forall i$.

4. Interaction energy formulation of non-uniform system

For the calculation of the entropy in the last section, the interaction potential between neighboring cells is overlooked. In this section, we will derive the interaction energy for a non-uniform system. As derived in [23], the interaction energy is calculated as

$$h_B = \sum_{i<j}^{K,K} \chi_{ij} c_i c_j, \tag{20}$$

where χ_{ij} indicates the interaction coefficient between two components. In the current work, we assume χ_{ij} to be constant for the sake of simplifying the model. This assumption is commonly adopted in established theories, such as regular solution theory and Flory-Huggins theory [24–27]. When χ_{ij} depends on the composition [28, 29], a similar strategy based on the Taylor expansion can be applied by using equation (10). For a non-uniform system, an infinitesimal element at the interface has a composition c_i and its boundary layers with compositions of c_i^- and c_i^+, as proposed in section 2. Following equation (20), we obtain the expression for the interaction energy density of a non-uniform system as

$$h_B = \frac{1}{2}\sum_{i<j}^{K,K}\left(\chi_{ij}c_i^- c_j^- + \chi_{ij}c_i^+ c_j^+\right). \tag{21}$$

By employing the Taylor expansion for the infinitesimal increment of composition, the interaction energy of a non-uniform system is rewritten as

$$\begin{aligned} h_B(\boldsymbol{c},\nabla\boldsymbol{c}) = \sum_{i<j}^{K,K}\Big[&\chi_{ij}c_i c_j + \chi_{ij}(\boldsymbol{\ell_j})^2 c_i\nabla^2 c_j + \chi_{ij}(\boldsymbol{\ell_i})^2 c_j\nabla^2 c_i \\ &+ \chi_{ij}(\boldsymbol{\ell_i}\cdot\boldsymbol{\ell_j})(\nabla c_i\cdot\nabla c_j)\Big]. \end{aligned} \tag{22}$$

When there is no composition gradient, the interaction energy given by equation (22) is consistent with equation (20). By integrating the interaction energy density over the domain Ω, we obtain the interaction energy functional as

$$\mathcal{H} = \int_\Omega h_B(\boldsymbol{c},\nabla\boldsymbol{c})\,\mathrm{d}\Omega. \tag{23}$$

Similarly, with the aid of divergence theorem and no-flux boundary condition, the final interaction energy functional is rewritten as

$$\begin{aligned} \mathcal{H} &= \int_\Omega\sum_{i<j}^{K,K}\Bigg[\chi_{ij}c_i c_j + \underbrace{\chi_{ij}(\boldsymbol{\ell_i}\cdot\boldsymbol{\ell_j})}_{=:\kappa_1^h}(\nabla c_i\cdot\nabla c_j) \\ &\quad - \left(\underbrace{\frac{\mathrm{d}\left(\chi_{ij}c_i\boldsymbol{\ell_j}^2\right)}{\mathrm{d}c_i} + \frac{\mathrm{d}\left(\chi_{ij}c_j\boldsymbol{\ell_i}^2\right)}{\mathrm{d}c_j}}_{=:\kappa_2^h}\right)(\nabla c_i\cdot\nabla c_j)\Bigg]\mathrm{d}\Omega \\ &= \int_\Omega\sum_{i<j}^{K,K}\left[\chi_{ij}c_i c_j + \chi_{ij}\left(\boldsymbol{\ell_i}\cdot\boldsymbol{\ell_j} - \boldsymbol{\ell_j}^2 - \boldsymbol{\ell_i}^2\right)(\nabla c_i\cdot\nabla c_j)\right]\mathrm{d}\Omega. \end{aligned} \tag{24}$$

It should be noted that both entropy and interaction energy exhibit non-local behavior due to their dependence on composition gradients. In the entropy density, only the term $(\nabla c_i)^2$ is present, as entropy considers the independence of each lattice without interactions between adjacent lattices. In contrast, the cross term $\nabla c_i\cdot\nabla c_j$ appears in the formulation of the interaction energy, reflecting the consideration of interactions between adjacent lattices. For the case of $i = j$, the interaction energy indicates the self-energy [30, 31]; the aspect of self-energy is not the focus of the current work and will not be discussed here. By incorporating the higher order interaction energy term, a natural extension of equation (22) is achieved through the utilization of the non-uniform composition $c_i \pm \nabla c_i\cdot\boldsymbol{\ell_i} + \nabla^2 c_i(\boldsymbol{\ell_i})^2$.

Finally, we obtain the chemical free energy functional of a non-uniform
system as

$$\begin{aligned} \mathcal{F} = \mathcal{H} - T\mathcal{S}_B &= \int_\Omega\Bigg\{\sum_{i<j}^{K,K}\left[\chi_{ij}c_i c_j + \left(\kappa_1^h - \kappa_2^h\right)\nabla c_i\cdot\nabla c_j\right] \\ &\quad + \frac{R_\mathrm{g}T}{\bar{v}}\sum_{i=1}^{K}\left[c_i\ln c_i + (\kappa_1^s - \kappa_2^s)(\nabla c_i)^2\right]\Bigg\}\mathrm{d}\Omega \\ &= \int_\Omega\Bigg\{\left[\sum_{i<j}^{K,K}\chi_{ij}c_i c_j + \frac{R_\mathrm{g}T}{\bar{v}}\sum_{i=1}^{K}c_i\ln c_i\right] \\ &\quad + \left[\sum_{i<j}^{K,K}\left(\kappa_1^h - \kappa_2^h\right)\nabla c_i\cdot\nabla c_j + \frac{R_\mathrm{g}T}{\bar{v}}\sum_{i=1}^{K}(\kappa_1^s - \kappa_2^s)(\nabla c_i)^2\right]\Bigg\}\mathrm{d}\Omega. \end{aligned} \tag{25}$$

This free energy formulation reveals that the free energy of a non-uniform system can be expressed as the sum of two terms: one is the bulk energy term related to the composition, and the other is the gradient energy term, which depends on the composition gradient. In a binary system, the cross term $\nabla c_i\cdot\nabla c_j$ can be replaced by the individual term $(\nabla c_i)^2$ based on the constraint: $c_1 + c_2 = 1$, indicating the consistency between our free energy formulation and the one proposed by Cahn and Hilliard (referencing the equation (2.6) in [16]). This substitution simplifies the expression and aligns with the symmetric nature of binary systems. However, in systems with more than two components (ternary or higher), the contribution from the cross terms $\nabla c_i\cdot\nabla c_j$ (where $i \neq j$) should be considered. These cross terms reflect the interactions and correlations between different composition gradients, which become increasingly important as the number of components increases.

5. Internal energy

In this section, we analyze the internal energy of a non-uniform system. When all components are fully miscible, the internal energy of this homogeneous system is formulated as

$$\begin{aligned} \mathcal{U} &= \int_\Omega u\,\mathrm{d}\Omega \\ &= \int_\Omega C_v(\boldsymbol{c})\,T\,\mathrm{d}\Omega, \end{aligned} \tag{26}$$

where $\boldsymbol{c}$ and T denote the uniform composition and uniform temperature of this system within the domain Ω, respectively. For a non-uniform system, the heat capacitance at the interface depends on the compositions c_i^- and c_i^+, and the internal energy of the non-uniform system is expressed as

$$\mathcal{U} = \frac{1}{2}\int_\Omega \sum_{i=1}^{K} \left[C_v\left(c_i^-\right) + C_v\left(c_i^+\right)\right] T\mathrm{d}\Omega.$$

With the Taylor expansion for the heat capacitance

$$\begin{aligned} C_v\left(c_i^\pm\right) &= C_v\left(c_i \pm \nabla c_i \cdot \boldsymbol{\ell}_i + \nabla^2 c_i \left(\boldsymbol{\ell}_i\right)^2\right) \\ &= C_v\left(c_i\right) + \frac{\partial C_v}{\partial c_i}\left[\pm\nabla c_i \cdot \boldsymbol{\ell}_i + \nabla^2 c_i \left(\boldsymbol{\ell}_i\right)^2\right] \\ &\quad + \frac{1}{2}\frac{\partial^2 C_v}{\partial c_i^2}\left[\pm\nabla c_i \cdot \boldsymbol{\ell}_i + \nabla^2 c_i \left(\boldsymbol{\ell}_i\right)^2\right]^2 \\ &\quad + \frac{1}{2}\frac{\partial^2 C_v}{\partial c_i \partial c_j}\left(\pm\nabla c_i \cdot \boldsymbol{\ell}_i + \nabla^2 c_i \left(\boldsymbol{\ell}_i\right)^2\right) \\ &\quad \times \left(\pm\nabla c_j \cdot \boldsymbol{\ell}_j + \nabla^2 c_j \left(\boldsymbol{\ell}_j\right)^2\right) + \cdots, \end{aligned} \tag{27}$$

we obtain the following expression for the internal energy of a non-uniform system

$$\begin{aligned} \mathcal{U} = \int_\Omega \Bigg\{ &\sum_{i=1}^{K}\left[C_v\left(c_i\right) + \frac{\partial C_v}{\partial c_i}\left(\boldsymbol{\ell}_i\right)^2 \nabla^2 c_i + \frac{1}{2}\frac{\partial^2 C_v}{\partial c_i^2}\left(\boldsymbol{\ell}_i\right)^2 \left(\nabla c_i\right)^2\right] \\ &+ \sum_{i<j}^{K,K} \frac{1}{2}\frac{\partial^2 C_v}{\partial c_i \partial c_j}\left(\boldsymbol{\ell}_i \cdot \boldsymbol{\ell}_j\right)\left(\nabla c_i \cdot \nabla c_j\right)\Bigg\} T\mathrm{d}\Omega. \end{aligned} \tag{28}$$

By applying the divergence theorem and no-flux boundary condition, the internal energy of a non-uniform system can be reformulated as

$$\begin{aligned} \mathcal{U} = \int_\Omega \Bigg\{ &\sum_{i=1}^{K}\left[C_v\left(c_i\right) - \frac{1}{2}\frac{\partial^2 C_v}{\partial c_i^2}\left(\boldsymbol{\ell}_i\right)^2 \left(\nabla c_i\right)^2\right] \\ &+ \sum_{i<j}^{K,K} \frac{1}{2}\frac{\partial^2 C_v}{\partial c_i \partial c_j}\left(\boldsymbol{\ell}_i \cdot \boldsymbol{\ell}_j\right)\left(\nabla c_i \cdot \nabla c_j\right)\Bigg\} T\mathrm{d}\Omega. \end{aligned} \tag{29}$$

6. Elastic energy

For a uniform system, the classical theory of elasticity, such as Hooke's law, can be used to calculate the elastic energy. However, in a non-uniform system, these conventional principles cannot be directly applied due to the inhomogeneity of physical properties. In this section, we develop the formulation for the elastic energy in a non-uniform system.

The elastic energy for a unit volume is expressed as

$$f_\mathrm{E} = \frac{1}{2}\boldsymbol{\epsilon} : \boldsymbol{C}\left(\boldsymbol{c}\right) : \boldsymbol{\epsilon}, \tag{30}$$

where $\boldsymbol{C}$ is the stiffness tensor related to the composition and $\boldsymbol{\epsilon}$ represents the strain tensor. By integrating over the whole domain Ω, we obtain the elastic energy functional

$$\mathcal{F}_\mathrm{E} = \int_\Omega \frac{1}{2}\boldsymbol{\epsilon} : \boldsymbol{C}\left(\boldsymbol{c}\right) : \boldsymbol{\epsilon}\,\mathrm{d}\Omega. \tag{31}$$

For a non-uniform system, in the similar manner, we substitute the composition at interface $c_i^\pm$ into equation (31) and obtain

$$\mathcal{F}_\mathrm{E} = \int_\Omega \frac{1}{2}\sum_{i=1}^{K}\left[\frac{1}{2}\boldsymbol{\epsilon} : \boldsymbol{C}\left(c_i^-\right) : \boldsymbol{\epsilon} + \frac{1}{2}\boldsymbol{\epsilon} : \boldsymbol{C}\left(c_i^+\right) : \boldsymbol{\epsilon}\right] \mathrm{d}\Omega. \tag{32}$$

Analogous to equation (27), with the Taylor expansion of the elasticity tensor, the final expression of the elastic energy for non-uniform system is written as

$$\begin{aligned} \mathcal{F}_\mathrm{E} = \int_\Omega \frac{1}{2}\boldsymbol{\epsilon} : \Bigg\{ &\sum_{i=1}^{K}\left[\boldsymbol{C}\left(c_i\right) - \frac{1}{2}\frac{\partial^2 \boldsymbol{C}}{\partial c_i^2}\left(\boldsymbol{\ell}_i\right)^2 \left(\nabla c_i\right)^2\right] \\ &+ \sum_{i<j}^{K,K} \frac{1}{2}\frac{\partial^2 \boldsymbol{C}}{\partial c_i \partial c_j}\left(\boldsymbol{\ell}_i \cdot \boldsymbol{\ell}_j\right)\left(\nabla c_i \cdot \nabla c_j\right)\Bigg\} : \boldsymbol{\epsilon}\,\mathrm{d}\Omega. \end{aligned} \tag{33}$$

7. Electric potential energy

Next, we scrutinize the cases where the system is placed in an electric field. In this case, we consider the induced electric potential energy functional $\mathcal{U}_\mathrm{E}$, which is described as [32]

$$\mathcal{U}_\mathrm{E} = \int_\Omega \frac{1}{2}\varepsilon\left(\boldsymbol{c}\right)\left|\boldsymbol{E}\right|^2 \mathrm{d}\Omega, \tag{34}$$

where $\boldsymbol{E}$ is the electric field strength vector and $\varepsilon(\boldsymbol{c})$ denotes the material permittivity. We substitute the composition at the interface $c_i^\pm$ into equation (34) and integrate over the whole domain Ω, thereby obtaining electric energy formulation for a non-uniform system as

$$\mathcal{U}_\mathrm{E} = \int_\Omega \frac{1}{2}\left[\frac{1}{2}\sum_{i=1}^{K}\varepsilon\left(c_i^-\right)\left|\boldsymbol{E}\right|^2 + \frac{1}{2}\sum_{i=1}^{K}\varepsilon\left(c_i^+\right)\left|\boldsymbol{E}\right|^2\right] \mathrm{d}\Omega. \tag{35}$$

Analogously, we apply a Taylor expansion for the material permittivity and equation (35) can be reformulated as

$$\begin{aligned} \mathcal{U}_\mathrm{E} = \int_\Omega \frac{1}{2}\Bigg\{ &\sum_{i=1}^{K}\left[\varepsilon\left(c_i\right) - \frac{1}{2}\frac{\partial^2 \varepsilon}{\partial c_i^2}\left(\boldsymbol{\ell}_i\right)^2 \left(\nabla c_i\right)^2\right] \\ &+ \sum_{i<j}^{K,K} \frac{1}{2}\frac{\partial^2 \varepsilon}{\partial c_i \partial c_j}\boldsymbol{\ell}_i \cdot \boldsymbol{\ell}_j \nabla c_i \cdot \nabla c_j\Bigg\} \left|\boldsymbol{E}\right|^2 \mathrm{d}\Omega. \end{aligned} \tag{36}$$

8. Wall free energy

In the preceding discussion, we derived a general formulation of the energy functional for a non-uniform system, suitable for cases with a fluid–fluid interface, such as liquid–liquid or liquid–gas. However, in scenarios where the fluid phase contacts a solid wall, such as in wetting phenomena, the interaction energy between the solid substrate and the fluid remains an open question and is nearly impossible to measure by using traditional experimental methods. In our previous studies, we introduced a wall free energy to describe the energy contribution in the interface region between the substrate and the fluid, investigating the wetting phenomenon by incorporating this wall free energy into the phase-field model [33–36]. In the subsequent sections, we derive this wall free energy formulation based on the concept proposed in section 2.

When the fluid contacts a solid wall, the symmetry of the liquid near the solid substrate is disrupted. To address this, we partition the liquid into two distinct regions: the bulk region denoted as $\Omega(\boldsymbol{x})$ and an interface region that liquid directly interacts with the solid substrate A, defined as $\Gamma(\boldsymbol{x}) = \Omega \cap A$. Because of the wall effect, i.e. the interaction between the solid atom and the liquid molecules, the liquid composition on the substrate is not necessary to be the same as the one in the bulk away from the substrate. We denote the liquid composition in the interface region near the substrate as $\boldsymbol{c}(\boldsymbol{x})$, $\forall \boldsymbol{x} \in \Gamma$. The entropy in this region is the same as equation (19)

$$\mathcal{S} = \int_\Gamma -\frac{R_\mathrm{g}}{\bar{v}} \sum_{i=1}^{K} \left[c_i \ln c_i - \frac{1}{2c_i} \left(\boldsymbol{\ell}_i\right)^2 \left(\nabla c_i\right)^2 \right] \mathrm{d}\Gamma. \tag{37}$$

However, due to the asymmetry of the interaction, the interaction energy differs from the formulation of the bulk. We formulate the interaction energy as

$$\begin{aligned}\mathcal{H} = \int_\Gamma \Bigg\{ & \sum_{i<j}^{K,K} \left[\chi_{ij} c_i c_j + \chi_{ij} \left(\boldsymbol{\ell}_i \cdot \boldsymbol{\ell}_j - (\boldsymbol{\ell}_j)^2 - (\boldsymbol{\ell}_i)^2 \right) (\nabla c_i \cdot \nabla c_j) \right] \\ & + \sum_{i=1}^{K} \left[\chi_i c_i c_s + \chi_i \left(\boldsymbol{\ell}_i \cdot \boldsymbol{\ell}_s - (\boldsymbol{\ell}_s)^2 - (\boldsymbol{\ell}_i)^2 \right) (\nabla c_i \cdot \nabla c_s) \right] \Bigg\} \mathrm{d}\Gamma,\end{aligned} \tag{38}$$

where χ_i is the interaction coefficient between the ith component in liquid and solid substrate, and $\boldsymbol{\ell}_s$ indicates the characteristic length vector of the solid substrate.

Finally, we obtain the energy functional

$$\begin{aligned}\mathcal{F} &= \mathcal{H} - T\mathcal{S} \\ &= \int_\Gamma \Bigg\{ \sum_{i<j}^{K,K} \left[\chi_{ij} c_i c_j + \chi_{ij} \left(\boldsymbol{\ell}_i \cdot \boldsymbol{\ell}_j - (\boldsymbol{\ell}_j)^2 - (\boldsymbol{\ell}_i)^2 \right) (\nabla c_i \cdot \nabla c_j) \right] \\ &\quad + \sum_{i=1}^{K} \Bigg[\left(\chi_i c_i c_s + \chi_i \left(\boldsymbol{\ell}_i \cdot \boldsymbol{\ell}_s - (\boldsymbol{\ell}_s)^2 - (\boldsymbol{\ell}_i)^2 \right) (\nabla c_i \cdot \nabla c_s) \right) \\ &\quad + \frac{R_\mathrm{g} T}{\bar{v}} \left(c_i \ln c_i - \frac{(\boldsymbol{\ell}_i)^2}{2c_i} \left(\nabla c_i\right)^2 \right) \Bigg] \Bigg\} \mathrm{d}\Gamma.\end{aligned} \tag{39}$$

However, in general, the width of the solid–fluid interface is very thin and not comparable to the width of the interface for liquid–liquid or liquid–gas [37], i.e., $\boldsymbol{\ell}_s << \boldsymbol{\ell}_i$. Therefore, a multi-scale system occurs, when a non-uniform liquid is placed on a substrate. The mismatch of scales can lead to several potential issues when applying this wall energy formulation to study the wetting phenomenon in this multi-scale system: (I) Multi-scale systems often require significant computational resources to solve, especially when a fine-scale phenomenon needs to be resolved over large-scale domains. (II) Ensuring numerical stability and convergence can be difficult, particularly when dealing with disparate scales. (III) Parameters used in the equations might be scale-dependent, leading to inconsistencies when applying them across different scales. Additionally, in the aforementioned derivation, the variation of the composition across the interface is expressed by a smooth monotone function. While this selection is mathematically elegant, it is somewhat artificial. The true nature of how the composition varies across the interface region remains an open question. For instance, as shown in figure 2(b), the yellow line corresponds to a non-monotonic composition profile, such as that of a surfactant; the blue step-like curve depicts the case with a very thin interface, where the composition variation exhibits non-continuum properties. To overcome these limitations, an alternative method is used to formulate the wall free energy. Wang and Nestler [38] express this energy as a function of the average composition, also known as surface composition, within the substrate–fluid interface region, rather than relying on the local composition and composition gradient. Figure 2(a) illustrates a sketch for the composition concept near the substrate, when a non-uniform liquid interacts with a solid substrate. The blue circles represent elements of the solid substrate, while the mixed elements of the liquid are marked by yellow and blue particles. The dark-gray region denotes the bulk region of the substrate, and the light-gray region indicates the substrate–liquid interface. The composition profile of an exemplary ith component c_i is shown in figure 2(b) by a green line. In this alternative method, we denote the width of this substrate–liquid interface as, which is typically determined based on experimental measurements. The value of λ is generally on the order of a few angstroms to a few nanometers [39, 40]. An average composition of ith component $\bar{c}_i$ is used to represent its composition within this area. The wall free energy can thus be written as

$$\mathcal{F}_\mathrm{W} = \int_{\Gamma'} \lambda \left\{ \sum_{i=1}^{K-1} \left[u_i^0 \bar{c}_i + \frac{R_\mathrm{g} T}{\bar{v}} \bar{c}_i \ln \bar{c}_i \right] + \sum_{i<j}^{K-1,K-1} \chi_{ij} \bar{c}_i \bar{c}_j \right\} \mathrm{d}\Gamma'. \tag{40}$$

It should be noted that the diffuse-interface region Γ is treated as a sharp-interface boundary Γ'. u_i^0 denotes the internal energy of the pure substance of the ith component. The average composition $\bar{c}_i$ is determined by minimizing the interfacial energy $\mathcal{F}_\mathrm{W}$. In this way, the wall energy density is defined as

$$\gamma = \lambda \left\{ \sum_{i=1}^{K-1} \left[u_i^0 \bar{c}_i + \frac{R_\mathrm{g} T}{\bar{v}} \bar{c}_i \ln \bar{c}_i \right] + \sum_{i<j}^{K-1,K-1} \chi_{ij} \bar{c}_i \bar{c}_j \right\}. \tag{41}$$

It should be noted that the solid composition within the interface region is statistically constant and its variation within this region can be neglected in this approach. By utilizing the concept of average composition, we address the multi-scale system by describing the energy contribution of interfaces at different length scales with alternative approach differing from

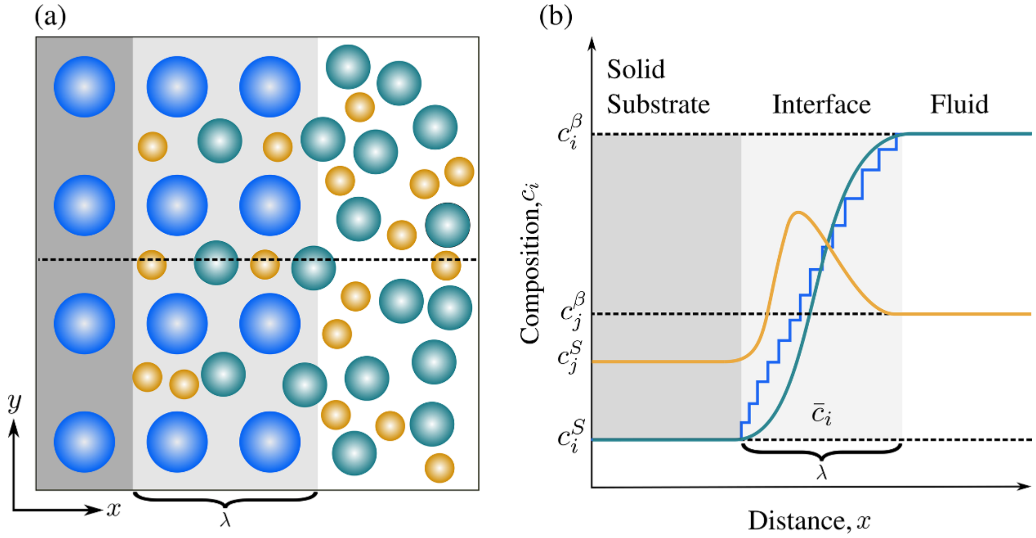

Figure 2. (a) Sketch for the composition concept near the substrate when the non-uniform system interacts with a solid substrate. The blue circles represent the elements in solid substrate and the mixing elements in non-uniform system are marked by yellow and dark-green circles. (b) The concentration profiles along the black dashed line in (a) are shown for three cases: (1) The green line represents a smooth monotone composition variation. (2) The yellow line corresponds to a non-monotonic composition profile, such as that of a surfactant. (3) The blue step-like curve depicts a very thin interface with non-continuum composition variation.

previous sections. This method circumvents the open question of how the composition of one component varies across the interface region.

9. Conclusion

In this study, we have proposed an alternative approach for deriving the free energy formulation of a non-uniform system. Our derivation begins with the reformulation of the local composition within the interface. Unlike the homogeneous composition in a uniform system, a composition gradient exists in the interface region of a non-uniform system. Therefore, we consider that the composition of the unit domain within the interface includes not only the bulk contribution but also an additional contribution from the boundaries of this unit domain. The composition is reformulated by incorporating first- and second-order infinitesimal increments.

By applying the reformulated local composition and the principles of statistical thermodynamics, we establish a formal expression for entropy related to composition and composition gradients. The development of the interaction energy formulation focuses on characterizing the energy contributions arising from interactions between different components in non-uniform systems. The integration of these entropy and interaction energy formulations leads to the construction of a comprehensive free energy expression that aligns with the work of Cahn and Hilliard.

Our approach, based on the reformulated local composition, involves establishing the entropy, interaction, and internal energy formulations to elucidate the physical significance of the free energy framework. The final free energy formulation for a non-uniform system is expressed as

$$\begin{aligned}\mathcal{F}=\mathcal{U}+\mathcal{H}-T\mathcal{S}=\int_\Omega\Bigg\{\sum_{i=1}^{K}\Bigg[&C_v\left(c_i\right)T-\frac{T}{2}\frac{\partial^2 C_v}{\partial c_i^2}\left(\boldsymbol{\ell}_i\right)^2\left(\nabla c_i\right)^2\\&+\frac{R_\mathrm{g}T}{\bar{v}}\left(c_i\ln c_i-\frac{1}{2c_i}\left(\boldsymbol{\ell}_i\right)^2\left(\nabla c_i\right)^2\right)\Bigg]\\&+\sum_{i<j}^{K,K}\Bigg[\frac{T}{2}\frac{\partial^2 C_v}{\partial c_i\partial c_j}\left(\boldsymbol{\ell}_i\cdot\boldsymbol{\ell}_j\right)\left(\nabla c_i\cdot\nabla c_j\right)+\chi_{ij}c_i c_j\\&+\chi_{ij}\left(\boldsymbol{\ell}_i\cdot\boldsymbol{\ell}_j-{\boldsymbol{\ell}_j}^2-{\boldsymbol{\ell}_i}^2\right)\left(\nabla c_i\cdot\nabla c_j\right)\Bigg]\Bigg\}\mathrm{d}\Omega.\end{aligned}\tag{42}$$

Complementing the work of Cahn and Hilliard, our alternative concept provides a comprehensive understanding for the construction of the free energy formulation, particularly in the context of diffuse interface models.

Furthermore, our concept can be applied to cases where other energy contributions exist in a non-uniform system. For applications in these cases, we derive formulations for two possible energy contributions in a non-uniform system, namely elastic energy and electric potential energy. These derivations are based on the concept of reformulating the local composition and applying the Taylor expansion for the infinitesimal increment of composition.

In the context of non-uniform fluids contacting solid substrates, as observed in wetting phenomena, we have reformulated the wall free energy to depend on the average composition within the substrate–fluid interface. This approach contrasts with traditional methods that depend on local composition and composition gradient. As derived in the last section, the wall free energy is reformulated as

$$\mathcal{F}_\mathrm{W}=\int_{\Gamma'}\lambda\left[\sum_{i=1}^{K-1}\left(u_i^0\,\bar{c}_i+\frac{R_\mathrm{g}T}{\bar{v}}\bar{c}_i\ln\bar{c}_i\right)+\sum_{i<j}^{K-1,K-1}\chi_{ij}\bar{c}_i\bar{c}_j\right]\mathrm{d}\Gamma'.\tag{43}$$

By employing this reformulated wall free energy, we can effectively address the multi-scale nature of a multicomponent system, which results from the different length scales between the substrate–fluid interface and the liquid–liquid or liquid–gas interfaces. This method circumvents the challenge of describing the composition variation of individual components across the interface region.

The new formulation proposed in this study enhances the modeling of non-uniform systems by offering a comprehensive representation of free energy that includes contributions from entropy, interaction energy, and internal energy. This approach is particularly advantageous for multicomponent systems and complex interfacial phenomena, as it provides a more accurate and flexible framework. The reformulation of wall free energy based on the concept of average composition simplifies the treatment of multiscale systems, addressing challenges inherent in traditional models. While the increased detail and flexibility improve the accuracy of simulations, they also introduce greater computational complexity and the need for careful parameter estimation. Despite these challenges, the proposed formulation represents a significant improvement over existing diffuse interface models, particularly in its ability to handle additional energy contributions and complex interface geometries.

We stress that the current work focuses on two key points: the introduction of an alternative concept for deriving the free energy formulation differing from Cahn & Hilliad and the reformulation of the wall free energy as a function of the average composition. By this way, we have proposed a novel and comprehensive understanding of the free energy formulation for non-uniform multicomponent systems.

Data availability statement

No new data were created or analyzed in this study.

Acknowledgments

The main part of the research has been carried out through funding by the German Research Foundation (DFG) within the frame of the Research Training Group 2561: Materials Compounds from Composite Materials for Applications in Extreme Conditions, which is gratefully acknowledged.

H D Zhang thanks for funding of the research through the Gottfried-Wilhelm Leibniz prize NE 822/31-1 of the German Research Foundation (DFG). F Wang is grateful to the VirtMat Project P09 of the Helmholtz Association (MSE-programme No. 43.31.01).

ORCID iD

Fei Wang https://orcid.org/0000-0003-3318-3264

References

[1] Young T 1805 Iii. an essay on the cohesion of fluids *Phil. Trans. R. Soc.* **95** 65–87
[2] Willard Gibbs J W 1878 On the equilibrium of heterogeneous substances *Am. J. Sci.* **3** 441–58
[3] Van der Waals J D 1979 The thermodynamic theory of capillarity under the hypothesis of a continuous variation of density *J. Stat. Phys.* **20** 200–44
[4] Tegze G, Pusztai T and Gránásy L 2005 Phase field simulation of liquid phase separation with fluid flow *Mater. Sci. Eng.* A **413** 418–22
[5] Luo Z, Du Y, Liu Y, Tang S, Pan Y, Mao H, Peng Y, Liu W and Liu Z 2018 Phase field simulation of the phase separation in the TiC-ZrC-WC system *Calphad* **63** 190–5
[6] Zhang H, Wu Y, Wang F, Guo F and Nestler B 2021 Phase-field modeling of multiple emulsions via spinodal decomposition *Langmuir* **37** 5275–81
[7] Zhang H, Wang F and Nestler B 2024 Electric-field induced phase separation and dielectric breakdown in leaky dielectric mixtures: Thermodynamics and kinetics *J. Chem. Phys.* **161**
[8] Cai Y, Wang F, Czerny A, Jürgen Seifert H J and Nestler B 2023 Phase-field investigation on the microstructural evolution of eutectic transformation and four-phase reaction in Mo-Si-Ti system *Acta Mater.* **258** 119178
[9] Kavousi S and Asle Zaeem M 2021 Quantitative phase-field modeling of solute trapping in rapid solidification *Acta Mater.* **205** 116562
[10] Cai Y, Wang F, Zhang Z and Nestler B 2021 Phase-field investigation on the peritectic transition in Fe-C system *Acta Mater.* **219** 117223
[11] Laxmipathy V Pavan, Wang F, Selzer M and Nestler B 2021 Phase-field simulations of grain boundary grooving under diffusive-convective conditions *Acta Mater.* **204** 116497
[12] Wu Y, Wang F, Huang W, Selzer M and Nestler B 2022 Capillary adsorption of droplets into a funnel-like structure *Phys. Rev. Fluids* **7** 054004
[13] Warren J A, Kobayashi R, Lobkovsky A E and Craig Carter W 2003 Extending phase field models of solidification to polycrystalline materials *Acta Mater.* **51** 6035–58
[14] Lobkovsky A E and Warren J A 2001 Phase-field model of crystal grains *J. Cryst. Growth* **225** 282–8
[15] William Cahn J and Miller Allen S 1977 A microscopic theory for domain wall motion and its experimental verification in Fe-Al alloy domain growth kinetics *J. Phys. Colloq.* **38** C7–51
[16] Cahn J W and Hilliard J E 1958 Free energy of a nonuniform system. I. Interfacial free energy *J. Chem. Phys.* **28** 258–67
[17] Plapp M 2015 Phase-field models *Handbook of Crystal Growth* 2nd edn, ed, editor T Nishinaga (Elsevier) ch 15, pp 631–68
[18] Ardell A J 2012 Gradient energy, interfacial energy and interface width *Scr. Mater.* **66** 423–6
[19] Brown H R 2001 Relation between the width of an interface between two polymers and its toughness *Macromolecules* **34** 3720–4
[20] Voci S and Dick J E 2023 An electrochemical perspective on the interfacial width between two immiscible liquid phases *Curr. Opin. Electrochem.* **39** 101244
[21] Kusaka R, Nihonyanagi S and Tahara T 2021 The photochemical reaction of phenol becomes ultrafast at the air–water interface *Nat. Chem.* **13** 306–11
[22] Pouryazdan M, Schwen D, Wang D, Scherer T, Hahn H, Averback R S and Bellon P 2012 Forced chemical mixing of immiscible Ag-Cu heterointerfaces using high-pressure torsion *Phys. Rev.* B **86** 144302

[23] Sundman B and Ågren J 1981 A regular solution model for phases with several components and sublattices, suitable for computer applications *J. Phys. Chem. Solids* **42** 297–301

[24] Gaskell D R and Laughlin D E 2017 *Introduction to the Thermodynamics of Materials* 6th edn (CRC Press)

[25] Flory P J 1953 *Principles of Polymer Chemistry* (Cornell University Press)

[26] Porter K E, Easterling D A and Easterling K E 2009 *Phase Transformations in Metals and Alloys (Revised Reprint)* 3rd edn (CRC Press)

[27] Wang F, Altschuh P, Ratke L, Zhang H, Selzer M and Nestler B 2019 Progress report on phase separation in polymer solutions *Adv. Mater.* **31** 1806733

[28] Potter C B, Davis M T, Albadarin A B and Walker G M 2018 Investigation of the dependence of the Flory–Huggins interaction parameter on temperature and composition in a drug–polymer system *Mol. Pharm.* **15** 5327–35

[29] Loo W S, Sethi G K, Teran A A, Galluzzo M D, Maslyn J A, Oh H J, Mongcopa K I and Balsara N P 2019 Composition dependence of the Flory–Huggins interaction parameters of block copolymer electrolytes and the isotaksis point *Macromolecules* **52** 5590–601

[30] Typel S 2005 Relativistic model for nuclear matter and atomic nuclei with momentum-dependent self-energies *Phys. Rev.* C **71** 064301

[31] Coffey D and Bedell K S 1993 Nonanalytic contributions to the self-energy and the thermodynamics of two-dimensional fermi liquids *Phys. Rev. Lett.* **71** 1043–6

[32] Zhang H, Wang F and Nestler B 2024 Multi-component electro-hydro-thermodynamic model with phase-field method. I. Dielectric *J. Comput. Phys.* **505** 112907

[33] Wu Y, Urrutia Gomez J E, Zhang H, Wang F, Levkin P A, Popova A A and Nestler B 2024 Digital twin of a droplet microarray platform: evaporation behavior for multiple droplets on patterned chips for cell culture *Droplet* **3** e94

[34] Zhang H, Wang F and Nestler B 2023 Line tension of sessile droplets: thermodynamic considerations *Phys. Rev.* E **108** 054121

[35] Wang F, Zhang H, Wu Y and Nestler B 2023 A thermodynamically consistent diffuse interface model for the wetting phenomenon of miscible and immiscible ternary fluids *J. Fluid Mech.* **970** A17

[36] Wang F and Nestler B 2021 Wetting transition and phase separation on flat substrates and in porous structures *J. Chem. Phys.* **154** 094704

[37] Nikolov S, Han C-S and Raabe D 2007 On the origin of size effects in small-strain elasticity of solid polymers *Int. J. Solids Struct.* **44** 1582–92

[38] Wang F and Nestler B 2024 Wetting and contact-angle hysteresis: density asymmetry and van der Waals force *Phys. Rev. Lett.* **132** 126202

[39] Gennes P-G, Brochard-Wyart F and Quéré D *et al* 2004 *Capillarity and Wetting Phenomena: Drops, Bubbles, Pearls, Waves* (Springer)

[40] Heslot F, Fraysse N and Cazabat A M 1989 Molecular layering in the spreading of wetting liquid drops *Nature* **338** 640–2